Simulation and Modeling of Nonlinear Magnetics

Mark C. Williams, Harris Semiconductor
Ronald S. Vogelsong, Harris Semiconductor
Kenneth S. Kundert, Cadence Design Systems

Abstract - A procedure for modeling and simulation of arbitrary nonlinear magnetics devices is presented. A set of electromagnetic primitives is described as implemented in SpectreHDL. The primitives include cores, gaps, and windings that are combined to model ferromagnetic inductors and transformers. A ferromagnetic core model based on the Jiles/Atherton algorithm [1][2] is described. The model is used to illustrate how to overcome some difficult modelling issues such as hysteresis, implicit equations, and multi-disciplinary models.

I. Introduction

Many designs for power applications, such as switching power supply and regulator circuits, make use of ferromagnetic inductors and transformers. These applications have created a need for a model that can accurately describe the operation of nonlinear magnetic devices. Unfortunately, these devices exhibit several qualities that make modeling difficult. In particular, the nonlinear hysteric nature and the wide variety of core topologies pose a challenge to generic modeling of such devices.

It is impractical to model all possible configurations with a single model topology. Instead, a transformer model of arbitrary complexity can be assembled using a small set of building blocks composed of windings, cores, and gaps.

This paper describes a methodology to represent nonlinear magnetics devices. Models are developed to describe the operation of each of the building blocks. Linear relationships are used to describe the winding and gap models. The theory behind the nonlinear core model is described in detail. Models for the ferromagnetic primitives are implemented in SpectreHDL. Finally, the results from a simulation of a transformer is presented.

II. Modeling Approach

Various transformer configurations can be modeled by treating the magnetic portion of the component as a circuit itself. The circuit consists of cores, gaps and windings interconnected in a topology that matches that of the component being modeled. The magnetic components relate magnetic force ($\mathcal{F}$) and flux (Φ). The cores and gaps are purely magnetic components, whereas the windings represent a coupling between the electrical and magnetic circuits.

Consider a transformer with four windings constructed in an **E** configuration with a gap in the center arm. Physically, the transformer is shown in Figure 1. Schematically, the same transformer is shown in Figure 2. C1, C2, and C3 represent core fragments that model the three arms of the **E** core. G1 represents the gap in the center arm and G2 represents the leakage through the air around the windings. W1, W2, W3, and W4 are the four windings.

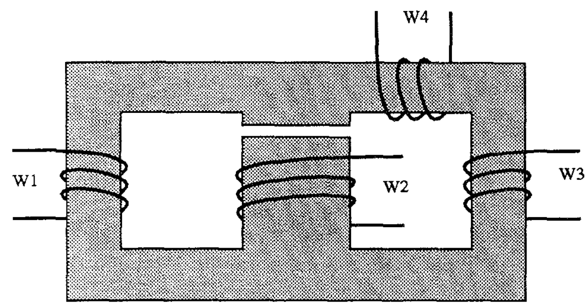

Figure 1. Physical Representation of an E Core.

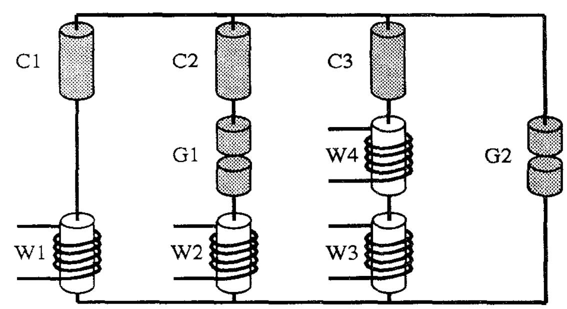

Figure 2. Topological Representation of an E Core.

III. Linear Magnetics Primitives

In order to understand the theory behind this algorithm, it is helpful to first review the relationships between the fundamental electric and magnetic quantities. Figure 3 depicts the relationships between each of the electrical quantities and the analogous relationships between their magnetic counterparts. The transformations between these two domains are defined by Faraday's Law and Ampere's Law.

A. The Gap Model

An air gap in a magnetic circuit is analogous to a linear resistor in an electrical circuit. It is represented by a linear reluctance, $\mathcal{R}$, that is a function of the cross-sectional area of the core, the gap length, and the permeability of free space, μ_0. From Figure 3, it is seen that the reluctance is the relationship between the magneto-motive force, $\mathcal{F}$, and the flux, Φ. The mathematical relationship is shown in Equation 1.

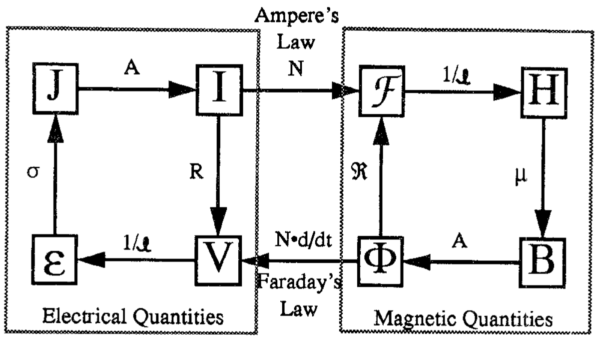

Figure 3. Relationships Between Electric and Magnetic Quantities.

$$\Re_G = \frac{\mathcal{F}}{\Phi} = \frac{l}{\mu_0 A} \tag{1}$$

B. The Winding Model

A winding couples the electrical and magnetic domains. The energy transferred between domains is scaled by the number of turns in the winding, N. The relationship from the electrical to the magnetic domain is defined by Ampere's Law as shown in Equation 2.

$$\mathcal{F} = NI \tag{2}$$

Similarly, the energy transfer from the magnetic back to the electrical domain is defined by Faraday's Law. In addition, the electrical winding can have a finite series resistance, R_W, defined by Ohm's Law. These effects are combined via superposition, resulting in the relationship shown in Equation 3.

$$V = R_W \cdot I + N\frac{d\Phi}{dt} \tag{3}$$

IV. Nonlinear Magnetics Theory

This section describes the underlying theory of the nonlinear behavior of ferromagnetic devices. The model is based on a phenomenological algorithm that emulates magnetic behavior using differential equation based mathematics.

While the magnetic quantities analogous to voltage (V) and current (I) are magneto-motive force ($\mathcal{F}$) and magnetic flux (Φ), the behavior of a saturable magnetic core is typically described in terms of its magnetic flux density (B) vs. magnetic field intensity (H). This relationship takes the form of a bistable sigmoid, as shown in Figure 4.

The relationship between B and H is defined by the permeability (μ) of the material. For magnetic materials, the permeability can be related to the permeability of free space (μ_0) by the relative permeability (μ_r). A particular class of magnetic materials (ferromagnetic) can exhibit variable nonlinear relative permeabilities. The relationships between these quantities is shown in Equation 4.

$$B = \mu H = \mu_0 \mu_r H = \mu_0 (H + M) \tag{4}$$

The parameter M in the equation refers to the magnetism or field intensity within the material that is contributed by the

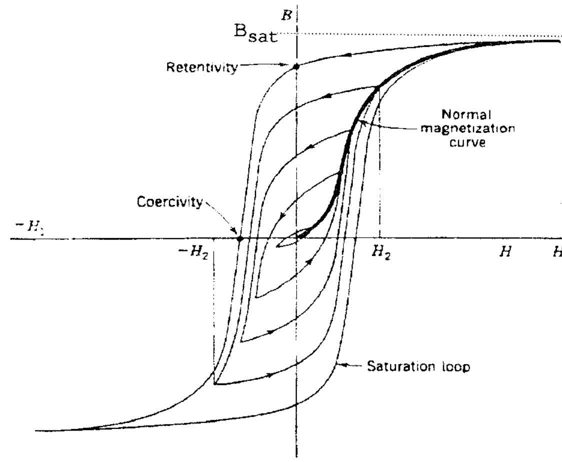

Figure 4. B vs. H Curve with Minor Loops. [4]

magnetic domains. The variation in permeability (μ) is a result of the changing magnetism (M) of the solid as energy from the applied field (H) is absorbed into the domains. Since the relative permeability (μ_r) is dependent on the ratio of applied and resident fields (magnetic susceptibility), the field density equation may be expanded into the more general relationship given by the final relationship, in which the relative permeability is incorporated into the internal field intensity component (M).

If a sample of magnetic material is examined on a per domain basis, the differential field strength around any given domain will be somewhat larger than expected due to its proximity to the remainder of the domains in the material. In effect, a given domain experiences the magnetic influence of the averaged total magnetism of the solid, since the orientation of any given domain may be random. At this point, it is appropriate to define an effective magnetic field intensity (H_{eff}), existing within the solid, that is the sum of the applied field (H) and some averaged contribution from the magnetism (M) of the surrounding domains. The proposed equation adjusts the percentage of bulk magnetism (M) added to the applied field intensity (H) through the scaling coefficient alpha (α) which typically has a value around 10^{-3}. The modified relationship for the magnetic field intensity experienced by a single domain is given by Equation 5.

$$H_{eff} = H + \alpha M \tag{5}$$

If a magnetic material was able to return all of the magnetic energy that was input, the resulting magnetization curve would take the form of a single valued sigmoid (equivalent to the center line of the hysteresis loop shown in Figure 4). This curve, referred to as the anhysteric magnetization curve, represents the ideal or lossless magnetization of a material. The function that was chosen to model this semi-empirical representation was developed by Langevin [5]. The parameters used to calculate this quantity are the effective field strength (H_{eff}) given by Equation 5, the saturation level (M_{sat}), and the shaping coefficient gamma (γ), which adjusts the slope of the curve according to the magnetic hardness of the material. The phenomenological representation of anhysteric magnetization (M_{anh}) proposed by Langevin is defined by Equation 6.

$$M_{anh} = M_{sat} \cdot \left(\coth\left(\frac{H_{eff}}{\gamma}\right) - \frac{\gamma}{H_{eff}} \right) \quad (6)$$

The total magnetic field in ferromagnetic materials can be separated into ideal and irreversible components, where the irreversible represents the energy dissipated in magnetizing the material. Jiles and Atherton formulated a model which expresses the total magnetization as a weighted average in the form shown in Equation 7.

$$M = cM_{anh} + (1-c) M_{irr} \quad (7)$$

The equation is composed of an anhysteric term which is a true function, in the mathematical sense, of the applied magnetic field (H) defined implicitly through the Langevin function, and an irreversible term which is a contribution computed through inexact differentials. The fundamental differential equation, proposed by Jiles and Atherton, is shown in Equation 8. The underlying theory is beyond the scope of this paper, but a more detailed derivation is given in the references [1][2].

$$M = M_{anh} - \delta k \frac{dM_{irr}}{dH_{eff}} \quad (8)$$

The equation consists of a magnetization term for the anhysteric component (representing the lossless term) and a magnetization term for the irreversible component that lumps the material dependent variation into a single term (k). The parameter delta (δ) can take on the values of either 1 or -1 depending on whether it is the positive or negative half cycle of input function, respectively. This equation can be converted to the standard differential notation by substituting Equation 5 into Equation 8 for the effective field (H_{eff}) and rearranging terms. The resulting form is shown in Equation 9.

$$\frac{dM_{irr}}{dH} = \frac{M_{anh} - M_{irr}}{\delta k - \alpha (M_{anh} - M_{irr})} \quad (9)$$

Equation 9 can be combined with Equation 7 to define the total differential susceptibility of the material. Integration of this quantity results in the total susceptibility (χ_m) which is defined as the ratio between M and H. Referring to Equation 4, the relative permeability (μ_r) can be alternately defined as shown in Equation 10.

$$\mu_r = \frac{M}{H} + 1 = \chi_m + 1 \quad (10)$$

Referring to Figure 3, the final relationship between magnetic flux (Φ) and magneto-motive force ($\mathcal{F}$) can now be defined as shown in Equation 11.

$$\Phi = BA = \mu_0 \mu_r AH = \mu_0 A (H + M) \quad (11)$$

The nonlinear reluctance ($\mathcal{R}$) of the core, equal to the reciprocal of susceptance (χ), is defined as the ratio between $\mathcal{F}$ and Φ, as shown in Equation 12.

$$\Re = \frac{1}{\chi} = \frac{\mathcal{F}}{\Phi} = \frac{l}{\mu A} = \frac{l}{\mu_0 A\left(1 + \frac{M}{H}\right)} \quad (12)$$

V. SpectreHDL Model

Three SpectreHDL modules were developed based on the theory derived in the previous sections. The gap, winding and core module definitions are listed in Tables 1, 2, and 3, respectively.

The SpectreHDL language provides pre-defined node/branch quantities of voltage (V) and current (I) in the electrical domain and magneto-motive force (MMF) and magnetic flux (Wb) in the magnetic domain. Functions by these names are used to access their respective quantities ($V(a,b)$ is the voltage between nodes a and b; $I(a)$ is the current into port a).

The air gap module in Table 1 is a direct implementation of the relationship shown in Equation 1. Note that the simplicity of this language allows for very concise specification of mathematical relationships. The ability to pass in arguments (*len* and *area*), with optional default values and bounds checking, allows for generic use of the module.

Table 1: Air Gap Module

```
module gap(p,n) (len, area)
node[MMF,Wb] p, n;
parameter real len=.1 from [0:inf);// eff.len.
parameter real area=1 from (0:inf);// area
{
    analog {
      MMF(p,n) <- len * Wb(p,n) / (u0 * area);
    }
}
```

The winding module in Table 2 directly implements the relationships defined by Equations 2 and 3 which couple the magnetic and electrical domains. Note that the *dot* operator is used to perform the time derivative.

Table 2: Electro-Magnetic Winding Module

```
module winding(e1,e2,m1,m2) (turns, r)
node[V,I] e1, e2;
node[MMF,Wb] m1, m2;
parameter real turns=1;
parameter real r=0;// winding resist. per turn
{
    analog {
     MMF(m1,m2) <- turns * I(e1,e2);
     V(e1,e2) <- turns * (r * I(e1,e2) -
                dot(Wb(m1,m2)));
    }
}
```

The *core* module in Table 3 defines the $\mathcal{F}$ vs. Φ relationship as a function of the parameters of the core. This module is implemented such that it can be shared between instances of each device. The arguments passed into the model (*len* and *area*) are specific to each instance, whereas the remaining parameter statements define defaults and bounds for the model parameters that are shared between instances.

Equation 9 describes the characteristics of the magnetic material in terms of incremental quantities, and so cannot be used directly in SpectreHDL. However, the equation can be converted into a useable form by first multiplying both sides by dH and integrating, then replacing dH with $(dH/dt)dt$:

$$M_{irr} = \int \frac{M_{anh} - M_{irr}}{\delta k - \alpha M_{anh} - M_{irr}} \dot{H} dt \quad (13)$$

Notice that this is an implicit equation, as M_{irr} appears on both sides of the equality. This presents no problem because SpectreHDL allows implicit formulations.

Table 3: Nonlinear Magnetic Core Module

```
module core(p,n) (len, area)
node[MMF,Wb] p, n;
parameter real len, area;
{
parameter real ms=1.6M from (0:inf);
parameter real a=1100 from (0:inf);
parameter real k=2000 from (0:inf);
parameter real alpha=1.6m from (0:inf);
parameter real c=0.2 from [0:1];
node [MMF,Wb] Hdot;   // internal Hdot nodes
export real H, B;    // flux intensity,density
real Manh, Mirr=0, dMirr, M, Heff, delta;
integer migrating;    // pinning site flag
   analog {
     H = MMF(p,n) / len;
     val(Hdot) <- dot(H);
     delta = sign(val(Hdot));
     B = Wb(p)/area;
     M = B/u0 - H;
     Heff = H + alpha * M;
     if (abs(Heff) > 0.001 * a)
         Manh = ms * (coth(Heff/a) - a/Heff);
     else
         Manh = ms * Heff/(3.0*a);
     dMirr = (Manh - Mirr)/(delta*k -
             alpha*(Manh - Mirr)) * val(Hdot);
     migrating = (delta > 0) ^ (M > Manh);
     Mirr = integ( migrating * dMirr, Manh );
     M = (1-c)*Mirr + c*Manh;
     Wb(p,n) <- area*u0*(H+M);
  }
}
```

There are a few aspects of this implementation that should be explained. First, $\mathcal{F}$ = *MMF(p,n)* and ϕ = `Wb (p)` = `Wb (p, n)`. Second, to avoid division by zero in Equation 6 when H_{eff} is near zero, it is replaced by the first term in its Taylor series expansion when $|H_{eff}| < \alpha/1000$. The ^ operator is the logical exclusive or operator, so *migrating* is true if $\delta > 0$ and $M > M_{anh}$ or if $\delta < 0$ and $M < M_{anh}$ (this clause was included to define the relaxation from the loop tips back toward the anhysteric to be fully reversible). Finally, *integ* computes the time-integral of its first argument, and the second argument specifies the initial value of the integral.

VI. Results

The electromagnetic circuit in Figure 2 was simulated using SpectreHDL with a sinusoidal excitation applied to the primary winding and appropriate loads on the remaining windings. The resulting input and output current waveforms are shown in Figure 5. The electrical characteristics clearly show the nonlinearity of the current s in the primary and tertiary windings and the relatively linear response of the secondary, due to the presence of the gap.

The magnetic flux density vs. field intensity displayed in Figure 6 shows the initialization curve, starting from an unmagnetized state, followed by the saturated (outer) hysteresis loop. The sinusoidal input magnitude was then linearly decreased with time to generate the remainder of the minor loops shown in the figure.

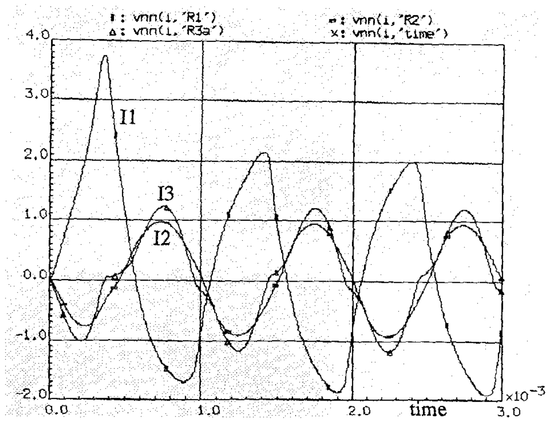

Figure 5. Graph of Winding Currents vs. Time.

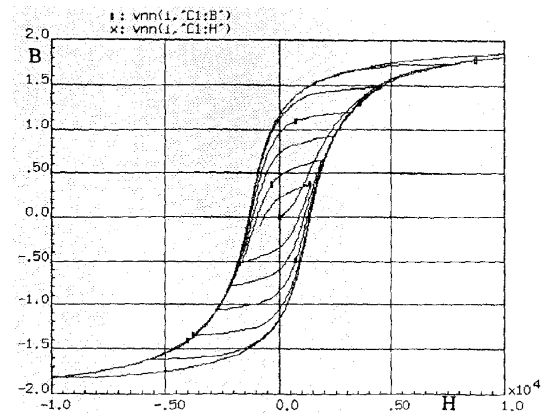

Figure 6. Graph of B vs. H, Including Minor Loops.

VII. Conclusions

In this paper, we described a methodology for modeling arbitrarily complex electromagnetic components by combining primitive magnetic and electromagnetic elements. In addition, an implementation of the complex Jiles-Atherton core model was described. Several difficulties inherent in this implementation were overcome. Transformation of the incremental model into an integro-differential time domain description provided a rational means for developing a simulation model. The use of SpectreHDL significantly simplified the actual implementation, due to its natural handling of the implicit formulation of the model.

VIII. . References

[1] Williams, M. C., "A CAD Model for Nonlinear Magnetics", Master's Thesis, University of South Florida, April 1994.

[2] Jiles, D. C. and D. L. Atherton, "Theory of Ferromagnetic Hysteresis," Journal on Magnetism and Magnetic Materials, 61, (1986): 48.

[3] SpectreHDL Reference Manual (Cadence Design Systems, San Jose, California, April 1994).

[4] Kraus, J. D. and Keith R. Carver. Electromagnetics. 2nd ed. New York: McGraw-Hill, 1973: 232.

[5] Langevin, M., Ann. de Chemistry et Physics., 5, (1905): 70.